Long-lived coherences for line-narrowing in high-field NMR

Riddhiman Sarkar [a,b], Puneet Ahuja [b,*], Paul R. Vasos [b,c], Aurélien Bornet [b], Olivier Wagnières [b], Geoffrey Bodenhausen [b,d,e,f]

[a] School of Chemistry, University of Southampton, Southampton SO17 1BJ, England
[b] Institut des Sciences et Ingénierie Chimiques, Ecole Polytechnique Fédérale de Lausanne, EPFL, Batochime, 1015 Lausanne, Switzerland
[c] Université Paris Descartes, UMR 8601 CNRS, 45, rue des Saints Pères 75006, Paris, France
[d] Université Pierre-et-Marie Curie, Paris, France
[e] Département de Chimie, Ecole Normale Supérieure, 24 Rue Lhomond, 75231, Paris Cedex 05, France
[f] CNRS, UMR 7203, France

ARTICLE INFO

Contents

1. Introduction

In conventional nuclear magnetic resonance spectroscopy (NMR), there is a well-known cascade of causes that lead to line-broadening effects: the larger the size of the molecules under investigation, the slower the rotational diffusion, the stronger the low-frequency components of the spectral density functions, the faster the transverse relaxation, hence the broader the spectral lines. This not only holds for 'conventional' spectroscopy of allowed transitions, i.e., for the observation of single-quantum transitions, but also for zero- and multiple-quantum spectra. The line broadening associated with slow tumbling makes NMR of large molecules and supramolecular assemblies difficult.

If we consider a pair of coupled spin-½ nuclei I and S that are reasonably isolated from unpaired electrons and other nuclei with significant magnetic moments, the longitudinal ('spin-lattice') relaxation rate $R_1 = 1/T_1$ and the transverse ('spin–spin') relaxation

---

rate $R_2 = 1/T_2$ of single-quantum coherences (SQCs) are predominantly due to the dipolar interaction between the two 'active' spins I and S. It has recently been shown [1,2] that long-lived states (LLS) may be excited by inducing a difference between the population of the singlet state $|S_0>$ and the average population of the three triplet states (*vide infra*). LLS are, to a very good approximation, immune to the mutual dipolar relaxation between the two 'active' spins, so that their life-times T_{LLS} can in principle be indefinitely long, at any rate much longer than T_1. In practice, a factor $T_{LLS}/T_1 > 37$ has been obtained for protons in favourable cases [3]. In nitrous oxide (N_2O) enriched in ^{15}N, a LLS comprising two ^{15}N nuclei can be sustained for several minutes [4]. Such long lifetimes of populations make it possible to extend the time scales over which phenomena such as slow exchange and slow translational diffusion may be characterised by NMR.

Extending the life-times of *coherences* will produce better-resolved spectra. Thus, by using spin echoes to achieve time-reversal [5,6], one can reduce *inhomogeneous* broadening, thus revealing the underlying homogeneous widths, i.e., the line-widths that would be observed in a perfectly homogeneous field. Achieving further narrowing is a greater challenge. Homogeneous broadening results from transverse relaxation, which is due to stochastic interactions that cannot be eliminated by the experimentalist.

In some fortunate cases, mutual cancellation of these stochastic interactions can lead to line narrowing. For instance, if the interaction tensors have favourable relative orientations, the fluctuations of dipole–dipole interactions and anisotropic chemical shifts can partially cancel each other, a phenomenon which is used in Transverse Relaxation Optimised SpectroscopY (TROSY) [7–11]. Similar kinds of interferences between several dipolar interactions can also be observed in methyl groups [12]. These effects have brought major advances by increasing the size of proteins and protein complexes that are amenable to structural and dynamic studies by NMR.

This article shows how the use of *coherent superpositions* between singlet and triplet states, which we like to call long-lived coherences (LLCs) [13], can lead to a significant resolution enhancement in NMR spectroscopy. LLCs belong to the class of zero-quantum coherences (ZQCs). Transitions between singlet and triplet states, which belong to different irreducible representations of the permutation group, are normally symmetry-forbidden and therefore have vanishing transition probabilities. We shall see that under certain circumstances, it is easy to excite *coherences across forbidden transitions*. In the manner of two-dimensional (2D) spectroscopy, one can allow these coherences to undergo a precession under the effect of the Hamiltonian in a variable evolution interval t_1, prior to re-converting them into observable signals in a detection interval t_2.

Recently, Pileio, Carravetta and Levitt discussed similar transitions between symmetric and anti-symmetric states in a different context. In their ingenious experiments [14], the Zeeman polarised sample was removed adiabatically from the magnetic field. It is then possible to bring about a Rabi nutation of the two-level system comprising the singlet and central triplet states by irradiation with an electromagnetic field at extremely low frequency (ELF), typically on the order of a few tens of Hz [14]. It has been shown that this nutation can lead either to the inversion of the populations across the singlet–triplet transition or to the creation of a singlet–triplet coherence that oscillates at a frequency determined by the *J*-coupling constant.

There are several differences between 'ELF' and 'LLC' experiments. In the former case, the Hamiltonian is switched adiabatically [14], typically in the course of a few seconds, by shuttling the sample outside the B_0 field. The longitudinal relaxation may take its toll, particularly for protons in biological macromolecules, as evidenced by field-cycling 'relaxometry' experiments [15]. In ELF experiments, the desired coherence must then be excited by a slow Rabi nutation in low field, which in practice requires an ELF pulse on the order of a few seconds to obtain a nutation through an angle $\pi/2$. By contrast, in our high-field LLC experiments, the spin system must be prepared by semi-selective inversion of one or more chosen multiplets in the proton spectrum. This requires one or several *rf* pulses of few ms for a π nutation angle, much shorter than T_1, although some losses due to T_2 relaxation during the pulses cannot be excluded. After semi-selective inversion, a continuous *rf* field B_1 is suddenly switched on, superimposed on the high static B_0 field. This allows one to switch almost instantaneously (i.e., within a fraction of a μs) to the desired Hamiltonian that is symmetrical under the spin permutation.

In contrast to the populations of long-lived states (LLS), which decay monoexponentially, the time-dependence of LLCs is oscillatory and must be mapped point-by-point in the manner of two-dimensional (2D) spectroscopy. In NMR, the eigenbase can be changed simply by switching a radio-frequency (*rf*) field on or off: if the *rf* field is on, the states are either symmetric or anti-symmetric under a permutation of the spins; if it is switched off, the states have no permutation symmetry because the difference between their Larmor precession frequencies robs the spins of their equivalence.

Like the popular TROSY method, the persistence of LLCs presupposes the existence of reasonably isolated scalar-coupled two-spin sub-systems. Unlike TROSY, however, isotope labelling of nitrogen-15 or carbon-13 nuclei is not required for LLCs, and the beneficial effects do not require high static magnetic fields. The isolation of the sub-systems can be improved through partial deuteration. This can be achieved by procedures that are well known for biological molecules [12].

We have shown [13] that the lifetimes of LLCs are significantly less prone to homogeneous broadening than conventional single-quantum coherences. In addition – like other ZQCs – they are insensitive to inhomogeneous broadening. Therefore, LLC lifetimes can be significantly longer than the transverse relaxation times T_2 of single-quantum coherences that can be measured with spin-echo sequences, depending on the correlation time of rotational diffusion [16]. The extent of the resolution-enhancement effect can be described by the resolution-enhancement factor $\varepsilon = T_{LLC}/T_2 = \Delta v/\Delta v_{LLC}$.

Predictions based on Redfield theory show that $3 < \varepsilon < 9$, where the lower limit ($\varepsilon = 3$) concerns small molecules in the extreme narrowing regime ($\tau_c \ll 1/\omega_0$), and the upper limit ($\varepsilon = 9$) is relevant for slowly-tumbling macromolecules with $\tau_c \gg 1/\omega_0$ [16]. Slow oscillatory decays of LLCs, monitored by two-dimensional spectroscopy, lead to very narrow lines with half-widths at half-height $\Delta v_{LLC} = (\pi T_{LLC})^{-1} \ll \Delta v = (\pi T_2)^{-1}$. Here we report the observation of line-widths $\Delta v_{LLC} = 60$ mHz in 2,3,6-trichlorophenol in aqueous solution, where the resolution-enhancement factor is $\varepsilon \sim 2.4$. We have observed line-widths $\Delta v_{LLC} = 600$ mHz in ubiquitin [13] where the resolution-enhancement factor is $\varepsilon \sim 2.2$. In principle, if external relaxation mechanisms can be silenced, for example by replacing all protons in the vicinity by deuterons, a gain in line-width by a factor $\varepsilon \sim 9$ should be possible in macromolecules. In earlier work, we could only excite one LLC after the other in a selective fashion. Here, we show that we can also create and sustain several LLCs in parallel in different spin systems, such as different Gly residues in ubiquitin.

2. The tailored Hamiltonian

The Hamiltonian of a system comprising two coupled spins I = S = ½ in a high magnetic field B_0, with chemical shifts $v_{I,S} = -\gamma(1 - \sigma_{I,S})B_0/(2\pi)$ and a scalar coupling constant J can be expressed as usual in units of h:

$$H = v_I I_z + v_S S_z + J\vec{I} \cdot \vec{S} \tag{1}$$

Assuming without loss of generality that $v_I > v_S$, and defining $\Delta v_{IS} = v_I - v_S > 0$, the Hamiltonian can be truncated if the difference between the chemical shifts is much larger than the scalar coupling constant, $\Delta v_{IS} \gg |J|$,:

$$H = v_I I_z + v_S S_z + J I_z S_z \tag{2}$$

with an eigenbasis known as the *product base* (PB):

$$\Phi_{PB} = \{|\alpha\alpha\rangle, |\alpha\beta\rangle, |\beta\alpha\rangle, |\beta\beta\rangle\} = \{|\alpha_I\alpha_S\rangle, |\alpha_I\beta_S\rangle, |\beta_I\alpha_S\rangle, |\beta_I\beta_S\rangle\} \tag{3}$$

where $|\alpha_I\beta_S\rangle = |m_I = +1/2, m_S = -1/2\rangle$ etc. If the static field vanishes ($B_0 = 0$), i.e., if the sample is removed from the field, the two spins I and S become magnetically equivalent:

$$H = J\vec{I} \cdot \vec{S} \tag{4}$$

The eigenbasis of this Hamiltonian, which is known as the *singlet–triplet base* (STB), is appropriate to describe a pair of equivalent spins comprising three symmetric triplet states and one anti-symmetric singlet state:

$$\Phi_{STB} = \{|T_{+1}\rangle, |T_0\rangle, |S_0\rangle, |T_{-1}\rangle\} \tag{5}$$

where

$$T_{+1} = |\alpha\alpha\rangle; T_0 = N(|\alpha\beta\rangle + |\beta\alpha\rangle); S_0 = N(|\alpha\beta\rangle - |\beta\alpha\rangle); T_{-1} = |\beta\beta\rangle \tag{6}$$

and $N = 2^{-1/2}$.

The two spins I and S become magnetically equivalent if a continuous-wave (CW) radio-frequency (rf) with an amplitude $|v_1| = |-\gamma B_1/(2\pi)| \gg \Delta v_{IS}$ is applied and the rf carrier v_{RF} is placed half-way between the two chemical shifts,

$$v_{RF} = v_{av} = (v_I + v_S)/2. \tag{7}$$

A frame rotating at v_{av} leads to the Hamiltonian:

$$H = v_1(I_x + S_x) + J\vec{I} \cdot \vec{S} + \frac{\Delta v_{IS}}{2}(I_z - S_z). \tag{8}$$

The last term involves $(I_z - S_z)$, which does not commute with $(I_x + S_x)$ and can be neglected when $v_1 \gg \Delta v_{IS}$:

$$H = v_1(I_x + S_x) + J\vec{I} \cdot \vec{S}. \tag{9}$$

This Hamiltonian is obviously symmetric under a permutation of the spins I and S. Its basis, STB, is given by Eq. (5).

The conversion $\Phi_{PB} = V \cdot \Phi_{STB}$ is described by the matrix:

$$V = \begin{pmatrix} 1 & 0 & 0 & 0 \\ 0 & N & N & 0 \\ 0 & N & -N & 0 \\ 0 & 0 & 0 & 1 \end{pmatrix}, \tag{10}$$

with $V = V^{-1}$ and $N = 2^{-\frac{1}{2}}$. Products of Cartesian components of angular momentum operators ('product operators') can provide a convenient description of coherence transfer processes. They can be transformed from the PB into the STB:

$$B_{PB} = V^{-1} B_{STB} V. \tag{11}$$

The effective fields experienced by the spins I and S are tilted through angles $\theta_{I,S}$ with respect to the z axis if an rf field B_1 is applied at v_{av}, exactly half-way between the two chemical shifts:

$$\tan\theta_{I,S} = \frac{\pm 2|v_1|}{\Delta v_{IS}} \tag{12}$$

with $0 < \theta_{I,S} < \pi$. If $v_1 \gg \Delta v_{IS}$, $\theta_{I,S} \sim \pi/2$, hence $\sin\theta_{I,S} \approx 1$ and $\cos\theta_{I,S} \approx 0$.

When a continuous radio-frequency field B_1 is suddenly applied along the x-axis of the rotating frame, the eigenstates of the system change instantaneously from the product base Φ_{PB} to the singlet–triplet base Φ_{STB}. In the presence of an rf field,

the operators of spins $K = \{I, S\}$ are transformed into the tilted interaction frame by:

$$\begin{pmatrix} K'_x \\ K'_y \\ K'_z \end{pmatrix} = \begin{pmatrix} \cos\theta_k & 0 & -\sin\theta_k \\ 0 & 1 & 0 \\ \sin\theta_k & 0 & \cos\theta_k \end{pmatrix} \begin{pmatrix} K_x \\ K_y \\ K_z \end{pmatrix} \tag{13}$$

When $\theta_{I,S} \sim \pi/2$, this simply amounts to relabeling $K'_z \rightarrow K_x$.

3. Definition of long-lived coherences

A coherent superposition between the singlet and central triplet states, which we call Q_{LLC}, can be readily defined in the STB [3,13]:

$$Q_{LLC} = |S_0\rangle\langle T_0| + |T_0\rangle\langle S_0| \tag{14}$$

This can be converted into Cartesian angular momentum operators that are more familiar in the field of NMR [17]:

$$Q_{LLC} = I_x - S_x \tag{15}$$

Thus, when the continuous rf field is suddenly switched on, the difference $(I_x - S_x)$ in the product base Φ_{PB} is converted into off-diagonal elements between the states $|S_0\rangle$ and $|T_0\rangle$ in the singlet–triplet base Φ_{STB} (Table A2 in Appendix). These off-diagonal elements correspond to long-lived coherences (LLCs). In Table A3 (Appendix), it is shown how the matrix representations of a few populations and coherences in the singlet–triplet base Φ_{STB} can be expressed in the product base Φ_{PB}.

A density operator of the form Q_{LLC} in Eq. (15) commutes with the first term of the Hamiltonian in Eq. (9), but the second isotropic scalar coupling term causes it to undergo an evolution:

$$[I_x - S_x, \vec{I} \cdot \vec{S}] = i(2I_y S_z - 2I_z S_y) \tag{16}$$

Solving the Liouville–von Neumann equation [17] (without considering relaxation for the time being) allows the evolution of the LLC to be described, provided that the applied rf field has an amplitude that is much larger than the chemical shift difference of the two spins:

$$Q_{LLC}(t) = (I_x - S_x)\cos(2\pi Jt) + (2I_y S_z - 2I_z S_y)\sin(2\pi Jt) \tag{17}$$

Thus, the LLC oscillates at a frequency given by the scalar coupling.

4. Relaxation of long-lived coherences

In addition to the coherent effect of the scalar spin–spin interaction, the LLC decays through relaxation,

$$\frac{d}{dt}Q_{LLC} = -(R_{LLC} + i2\pi J)Q_{LLC} \tag{18}$$

The LLC oscillates with a frequency determined by the scalar coupling constant J (imaginary part), while the rate R_{LLC} (real part) governs the decay. The oscillation frequency of these coherences is independent of the chemical shifts, and, by extension, of the local value of the B_0 field, so that LLCs, like other zero-quantum coherences (ZQCs), are insensitive to inhomogeneous broadening. The lifetime $T_{LLC} = 1/R_{LLC}$ can be significantly longer than the transverse relaxation times $T_2 = 1/R_2$ of single-quantum coherences. In a system of two spin-½ nuclei I and S, the rate R_2 is predominantly determined by the dipolar interaction between these spins [18]:

$$R_2 = \left(\frac{b_{IS}^2}{20}\right)[9J(0) + 15J(\omega) + 6J(2\omega)] + R_2^{ext} \tag{19}$$

where $b_{IS} = -\frac{\mu_0}{4\pi}\frac{\gamma^2\hbar}{r_{IS}^3}$ is the strength of the homonuclear dipolar coupling, r_{IS} the distance between the spins I and S, $J(\omega) = \frac{\tau_c}{1+\omega^2\tau_c^2}$ the

spectral density function, i.e., the Fourier transform of the autocorrelation function that describes the rotational diffusion of the molecule, τ_c the rotational correlation time, and the other quantities have their usual meaning. The term R_2^{ext} comprises contributions from external random fields, anisotropic chemical shifts (CSA), and dipole–dipole (DD) interactions to remote spins.

In contrast to 'longitudinal' LLS, which are not affected by the dipolar interaction between the two spins I and S, the 'transverse' relaxation rate constant R_{LLC} under the homonuclear dipolar interaction is given by [13]:

$$R_{LLC} = \left(\frac{b_{IS}^2}{20}\right)[J(0) + 3J(\omega) + 6J(2\omega)] + R_{LLC}^{ext} \quad (20)$$

If the R_{LLC}^{ext} term is small, the LLC has a slower relaxation rate than single-quantum coherences in all motional regimes, i.e., for arbitrary molecular tumbling rates. The ratio is $T_{LLC}/T_2 = \varepsilon = 3$ in the fast-tumbling limit ($\tau_c \ll 1/\omega_0$), when the spectral densities are equal at all frequencies. This ratio increases to $\varepsilon = 9$ for slow tumbling ($\tau_c \gg 1/\omega_0$). Thus, if the R_{LLC}^{ext} terms may be neglected, the ratio of the transverse relaxation times should increase from $T_{LLC}/T_2 = \varepsilon = 3$ in small molecules to $T_{LLC}/T_2 = \varepsilon = 9$ in macromolecules, thus making the gain more significant for large molecules.

5. Designing suitable experiments

A pulse sequence suitable for exciting and detecting LLCs [13] is shown in Fig. 1. We shall provide a step-by-step description of the method.

In the beginning of the experiment, at point $\tau_{(1)}$ in the sequence, the density operator σ_1 comprises only populations in thermal equilibrium, conveniently described by the operators I_z and S_z in Table A1 (Appendix):

$$\sigma_1 = E/2 - a(I_z + S_z) - b(I_z - S_z) \quad (21)$$

where $a = h\nu_{av}/(4k_BT)$ and $b = h\Delta\nu_{IS}/(8k_BT)$ in the high-temperature limit, where the Boltzmann distribution is linear in $1/T$. Since the unity operator, E, does not affect the outcome of NMR experiments if thermal correction factors can be neglected [19], and since $b \ll a$, we set $a = 1$ for simplicity and truncate as usual:

$$\sigma_1 = (I_z + S_z). \quad (22)$$

A semi-selective $(\pi)_x$ pulse is applied only to spin S between $\tau_{(1)}$ and $\tau_{(2)}$:

$$R_{(1->2)} = \exp(-i\pi S_x), \quad (23)$$

so that the system at point $\tau_{(2)}$ is described by:

$$\sigma_2 = R_{(1->2)}\sigma_1 R_{(1->2)}^{-1} = I_z - S_z. \quad (24)$$

After applying a non-selective $(\pi/2)_y$ pulse to both spins:

$$R_{(2->3)} = \exp\left[-i\frac{\pi}{2}(I_y + S_y)\right] \quad (25)$$

one obtains:

$$\sigma_3 = R_{(2->3)}\sigma_2 R_{(2->3)}^{-1} = I_x - S_x. \quad (26)$$

Between points $\tau_{(3)}$ and $\tau_{(4)}$, a CW rf field is switched on, so that the eigenstates of the system are switched instantaneously to the symmetry-adapted states Φ_{STB}. As explained in Eq. (13), we can now rewrite the density operator during $\tau_{(4)}$, since $\theta_{I,S} \sim \pi/2$:

$$\sigma_4 = I_x - S_x = I_z' - S_z'. \quad (27)$$

Table A2 shows how the matrix representation of the density operator σ_4 in the product base Φ_{PB} can be transformed into the singlet–triplet base Φ_{STB}:

$$\sigma_4 = I_z' - S_z' = |S_0><T_0| + |T_0><S_0|. \quad (28)$$

6. Long-lived coherences in a small molecule

In 2,3,6-trichlorophenol in a field $B_0 = 9.4$ T (400 MHz for protons) at room temperature, a ratio $\varepsilon = T_{LLC}/T_2 \sim 2.4$ has been observed, i.e., a resolution enhancement by a factor 2.4. It follows from Eq. (20) that ε is attenuated by uncorrelated external contributions to the relaxation rates. In analogy to relaxation rates R_{LLS} of long-lived states, which are immune to fluctuations associated with CSA and DD tensors that are symmetrical under permutation of spins I and S [20,21], the lifetimes of long-lived coherences will be affected to a lesser extent by spin-permutation symmetric relaxation mechanisms.

The coherent and relaxation properties of LLCs lead to 2D spectra with very high resolution, which can be used either to resolve nearly-degenerate signals or to measure J-couplings (and residual dipolar splittings in weakly oriented phases) with an unprecedented
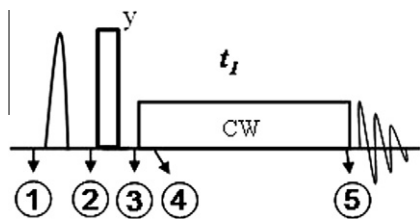

Fig. 1. Basic experiment used for excitation, sustaining and detection of long-lived coherences (LLCs) for one pair of spins at a time. The numbers in circles are mentioned in the equations. The open rectangle represents a non-selective $\pi/2$ pulse. All pulses are applied along the x axis. A typical π pulse for semi-selective inversion has a sinc shape, a length of 70 ms, and a peak rf amplitude of 40 Hz.
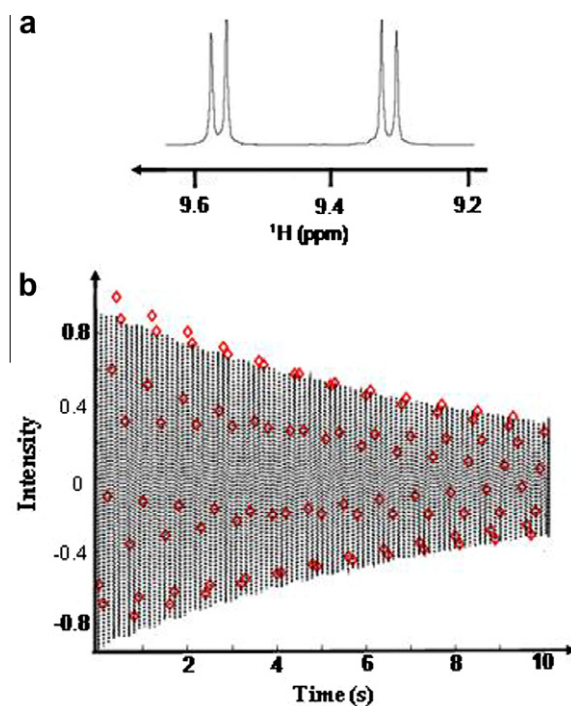

Fig. 2. (a) Proton spectrum of the two weakly coupled protons in 2,3,6-trichlorophenol at 400 MHz. (b) The experimental intensities (red lozenges) were plotted as a function of time t_1 and fitted with a function $I(t_1) = I_0 \cos(2\pi Jt_1)\exp(-R_{LLC}t_1)$. The best-fit parameters were $J = 8.760 \pm 0.001$ Hz and $R_{LLC} = 0.10 \pm 0.01$ s^{-1}. The amplitude of the continuous rf irradiation was 2.5 kHz. Each experiment was performed with four transients with a relaxation delay of 30 s. $J = 8.8$ Hz was obtained from a conventional 1D spectrum (For interpretation of the references to colour in this figure legend, the reader is referred to the web version of this article).
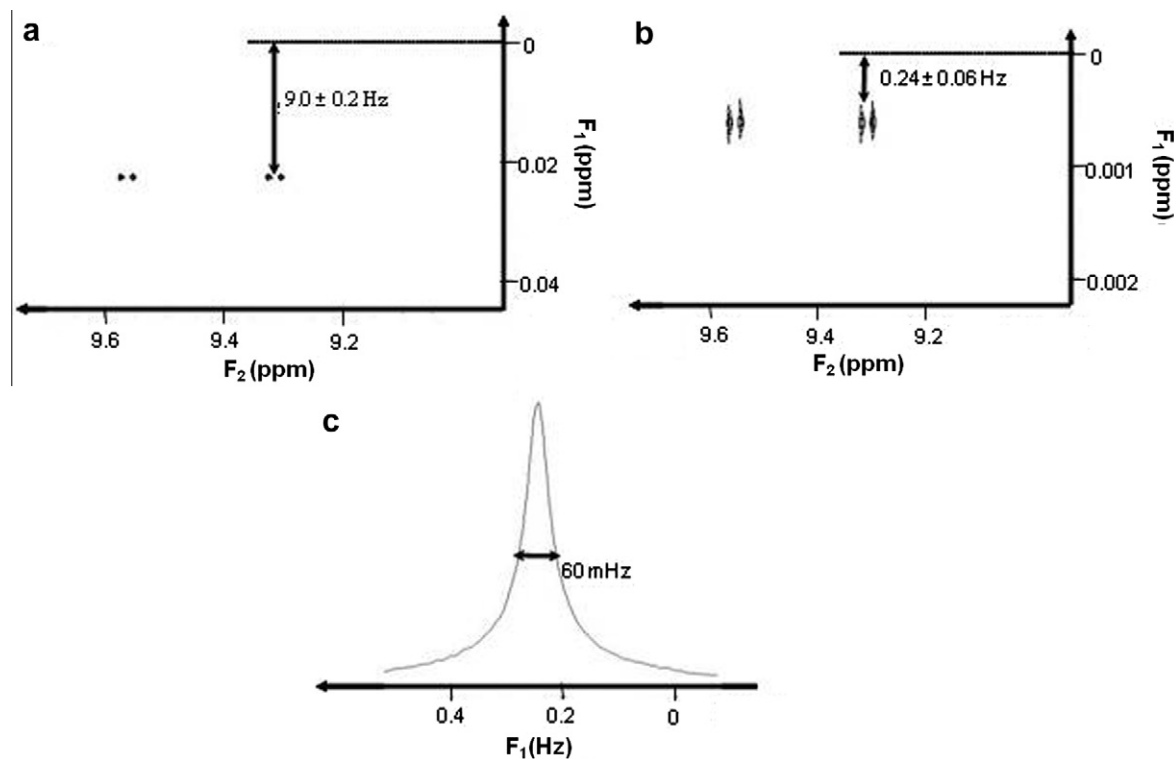
Fig. 3. (a) 2D spectra of 2,3,6-trichlorophenol at 400 MHz, where the chemical shifts and doublets appear in the ω_2 dimension and the J coupling in the ω_1 dimension. (b) Spectrum obtained with a spectral width reduced to 2 Hz in the ω_1 dimension by under-sampling in the t_1 dimension. The folded signals appear at a frequency of 0.24 Hz. Both 2D spectra were acquired in pure absorption mode using time-proportional phase increments (TPPI). (c) A column is extracted at $\omega_2 = 9.31$ ppm from the spectrum of Fig. 3b. The linewidth is merely 60 mHz in the ω_1 dimension.

accuracy in high field, albeit less accurately than in zero field [14]. The experiments were performed with the pulse sequence of Fig. 1. Fig. 2 shows the typical spectrum of two coupled spins-½, as well as the time-domain decay of LLCs in 2,3,6-trichlorophenol. In the 2D spectrum in Fig. 3a the chemical shifts are seen in the direct ω_2 dimension, whereas only a single peak at 9.0 ± 0.2 Hz is observed in the ω_1 dimension. This corresponds to the magnitude of the coupling constant J. Here, the ω_1 dimension was not sampled long enough to avoid truncation effects (t_1^{max} = 14.3 s with 1024 points and Δt_1 = 14 ms). To obtain the linewidth permitted by this method, one has to sample the indirect dimension as far as t_1^{max} = $5T_{LLC}$. The 2D spectrum in Fig. 3b was recorded by under-sampling the indirect dimension (t_1^{max} = 50 s with N_1 = 200 points and Δt_1 = 250 ms). The linewidth is only 60 mHz, unaffected by truncation. The spectral width was reduced to 2 Hz in the indirect dimension, so that the signal appeared at the (aliased) frequency v_1 = 0.24 Hz. The true frequency v_1 = J = 8.760 ± 0.001 Hz can be found by adding 4.5 times the spectral width.

7. Long-lived coherences in a protein

In the terminal residue Gly-76 of ubiquitin it was found that $\varepsilon = T_{LLC}/T_2$ = 2.2 [13]. The 2D experiment performed with the sequence of Fig. 1 in ubiquitin reveals chemical shifts and doublets in the ω_2 dimension, whereas only one frequency, which corresponds to the aliased J coupling, is detected in the ω_1 dimension. Under-sampling leads to spectral aliasing, but it is easy to correct for this effect and find that the aliased signal corresponds to J = −17.17 Hz. The full line-width at half-height of the signal was $\Delta v_{1/2}$ = 600 mHz in the ω_1 dimension, whereas the homogeneous linewidths of single-quantum coherences, estimated from a separate spin-locking $R_{1\rho}$-experiment, are $\Delta v_{1/2} \sim 1.4$ Hz.

8. Simultaneous excitation of several long-lived coherences

LLC experiments are not limited to studying one pair of spins after another. The semi-selective inversion of several spins in rapid succession (i.e., within an interval shorter than T_1) allows several LLCs to be excited simultaneously in different sub-systems. Here we demonstrate that LLCs can be excited simultaneously for the two C-terminal residues Gly-75 and Gly-76 in ubiquitin. We have designed the pulse sequence shown in Fig. 4a to achieve this. It is to be noted that there are three important differences between the simultaneous selection and selective methods for detecting LLCs. First, we have inserted a double-quantum (DQ) filter. Second, we need two semi-selective π pulses to invert two doublets. Third, the rf carrier was placed at the mean position between the two averages $v_{av}(I, S)$ and $v_{av}(I', S')$ of the four chemical shifts during the sustaining period. We used a train of sinc shaped pulses [22] to sustain the LLCs on both residues simultaneously because the use of a simple CW rf is not sufficient in this case. The oscillation frequency is not exactly equal to the scalar coupling, as the condition leading from Eq. (8) to Eq. (9) is not fully satisfied. However, the unaccounted coherent evolution terms in the Hamiltonian have a very limited effect (<1%, *vide infra*) in the precession rate of the coherences.

There are some new elements in Fig. 4a with respect to Fig. 1. Presaturation by a continuous-wave rf field ('CW' in Fig. 4a) was used to attenuate the water signal. A DQ filter was used to suppress perturbing multiplets with smaller splittings that arise from other spin systems in the protein. This filter consisted of a sequence of pulses, phase cycling to select the double-quantum coherence, pulsed field gradients, and matched delays τ = 1/(4J) = 14.7 ms, since |J| = 17 Hz for all glycine residues (irrespective of their environment). This filter creates pure in-phase coherences of the form $(I_x + S_x)$ for Gly-75 and Gly-76. Note that this filter also suppresses
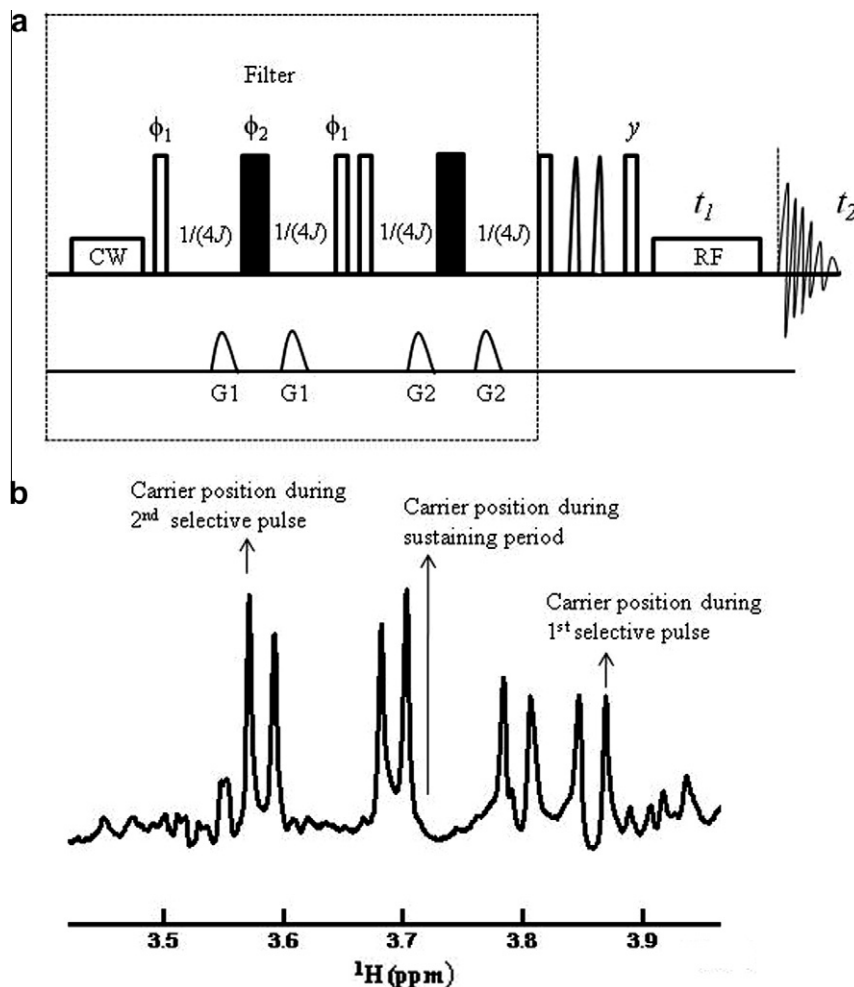
Fig. 4. Simultaneous excitation and observation of long-lived coherences (LLCs) in high magnetic fields, illustrated for a system with two pairs of diastereotopic protons, i.e., Gly-75 and Gly-76 in ubiquitin (a) The sequence is preceded by a double-quantum filter described in the text. Open and filled rectangles represent non-selective $\pi/2$ and π pulses, respectively. The narrow triangles represent semiselective inversion pulses. All pulses are applied along the x-axis, unless otherwise specified. The pulse phases were: $\phi_1 = x, y, -x, -y$; $\phi_2 = y, -x, -y, x$ and $\phi_{rec} = x, -x$. (b) Proton signals of Gly-75 and Gly-76 in ubiquitin obtained at 800 MHz with the pulse sequence (a) acquired after the DQ filter. The positions of the rf carrier at different time points are shown.

singlets quite efficiently. If no filters are used, the baseline of the LLC experiment can be contaminated by unwanted signals from residues other than glycines, which degrade the signal purity and render the fitting process inaccurate.

Fig. 5 shows signals of Gly-76 and Gly-75 in ubiquitin excited and observed with the simultaneous excitation method. Fitting yields modulation frequencies (which are not identical to the scalar coupling constants J, $vide$ $supra$) $v_1 = 17.20 \pm 0.01$ Hz for Gly-76 and $J = 16.80 \pm 0.05$ Hz for Gly-75. The relaxation rates were found to be $R_{LLC} = 2.1 \pm 0.1$ s^{-1} for Gly-76 and 2.1 ± 0.2 s^{-1} for Gly-75. These results were compared against standard, narrow-band LLC experiments in the manner of Fig. 1, performed separately for Gly-76 and Gly-75. The agreement between the two methods was found to be satisfactory. The 2D version of this LLC experiment is shown in Fig. 5b.

9. Conclusions

Remarkably narrow lines can be obtained in solution-state NMR spectra in high fields by exploiting the long life-times associated with superpositions of quantum states with different symmetry, known as long-lived coherences (LLCs). These can be compared with coherences that can be excited by extremely low frequency (ELF) irradiation in a vanishing static field. In high fields, LLCs can be excited almost instantaneously by spin-locking after a semi-selective population inversion. LLCs may be regarded as a special class of zero-quantum coherences (ZQCs). The slow oscillatory decays of long-lived coherences, which are characterised by decay constants T_{LLC} that can be on the order of 5 s in our examples, yield spectra with line-widths Δv_{LLC} on the order of 60 mHz. Scalar coupling constants and residual dipolar couplings (RDCs) can be, therefore, determined with unprecedented accuracy. The slow decay rates are very sensitive to extraneous relaxation mechanisms such as those arising from dilute paramagnetic impurities. In small molecules in the extreme narrowing limit, the line-widths Δv_{LLC} can be a factor 3 narrower than in spectra of ordinary single-quantum coherences (SQCs), provided relaxation is driven only by the dipole–dipole interaction between the two spins that participate in the LLC. In the slow motion limit for large molecules, the improvement in line-widths can in principle be a factor 9 in favourable cases, provided that extraneous relaxation mechanisms do not operate. This opens perspectives of studying molecular assemblies that are almost an order of magnitude larger than was hitherto possible. Generalisations to various other forms of spectroscopy other than NMR are conceivable if some means can
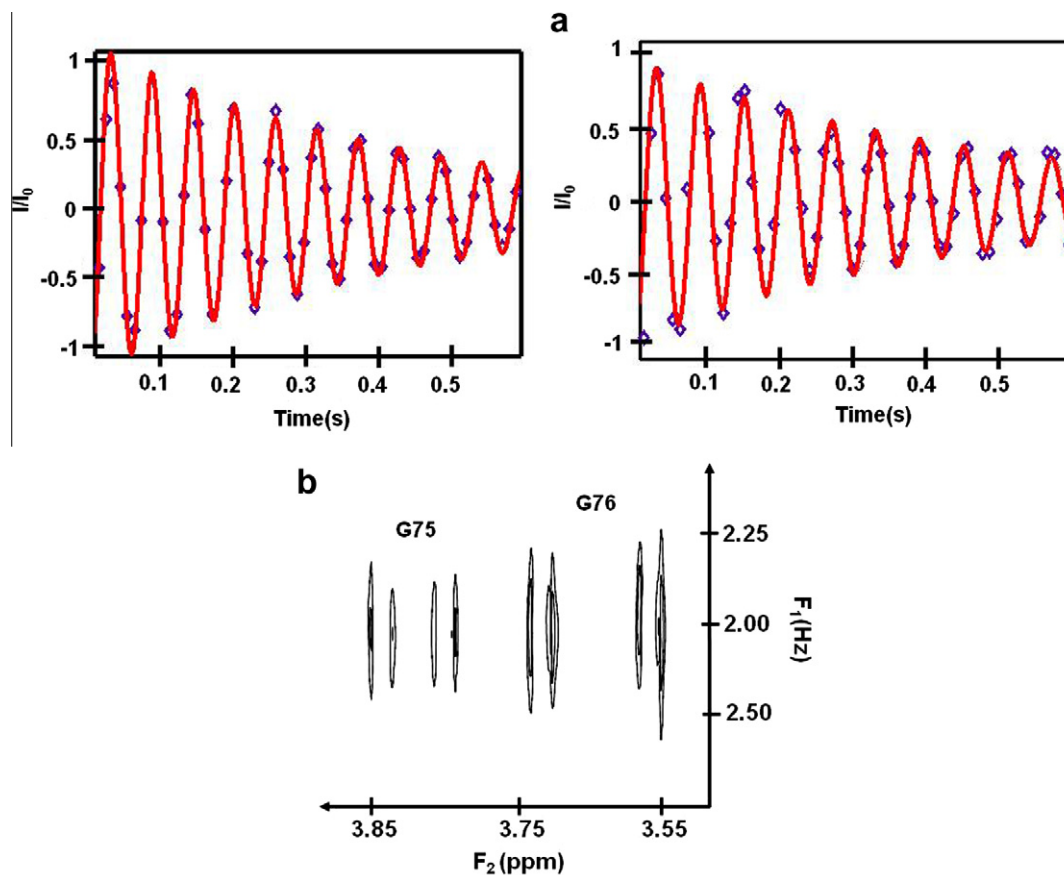
Fig. 5. Simultaneous excitation and observation of two LLCs in the C-terminal Gly-76 and Gly-75 residues of ubiquitin. (a) LLC decays of G76 and G75, as a function of the evolution interval t_1 at 600 MHz. (b) 2D LLC spectrum (processed in magnitude mode in the F_1 dimension) showing the signals arising from G75 and G76 of ubiquitin at 800 MHz. The LLCs were sustained by a sequence of contiguous sinc pulses, each of 1.2 ms length with a peak amplitude of 2.5 kHz. The *rf* carrier was placed at the mean position between the four chemical shifts of the two residues. The π pulses for semi-selective inversion had a sinc shape, a length of 70 ms, and a peak *rf* amplitude of 40 Hz.

Table A1

A selection of matrix representations of products of angular momentum operators for spin-½ nuclei in a two-spin system, expressed in the product base Φ_{PB} and in the singlet-triplet base Φ_{STB}.

Operator	In Φ_{PB}	In Φ_{STB}
I_z	$\frac{1}{2}\begin{pmatrix} 1 & 0 & 0 & 0 \\ 0 & 1 & 0 & 0 \\ 0 & 0 & -1 & 0 \\ 0 & 0 & 0 & -1 \end{pmatrix}$	$\frac{1}{2}\begin{pmatrix} 1 & 0 & 0 & 0 \\ 0 & 0 & 1 & 0 \\ 0 & 1 & 0 & 0 \\ 0 & 0 & 0 & -1 \end{pmatrix}$
S_z	$\frac{1}{2}\begin{pmatrix} 1 & 0 & 0 & 0 \\ 0 & -1 & 0 & 0 \\ 0 & 0 & 1 & 0 \\ 0 & 0 & 0 & -1 \end{pmatrix}$	$\frac{1}{2}\begin{pmatrix} 1 & 0 & 0 & 0 \\ 0 & 0 & -1 & 0 \\ 0 & -1 & 0 & 0 \\ 0 & 0 & 0 & -1 \end{pmatrix}$
I_x	$\frac{1}{2}\begin{pmatrix} 0 & 0 & 1 & 0 \\ 0 & 0 & 0 & 1 \\ 1 & 0 & 0 & 0 \\ 0 & 1 & 0 & 0 \end{pmatrix}$	$\frac{1}{2\sqrt{2}}\begin{pmatrix} 0 & 1 & -1 & 0 \\ 1 & 0 & 0 & 1 \\ -1 & 0 & 0 & 1 \\ 0 & 1 & 1 & 0 \end{pmatrix}$
$2I_yS_z$	$\frac{1}{2}\begin{pmatrix} 0 & 0 & -i & 0 \\ 0 & 0 & 0 & i \\ i & 0 & 0 & 0 \\ 0 & -i & 0 & 0 \end{pmatrix}$	$\frac{1}{2\sqrt{2}}\begin{pmatrix} 0 & -i & i & 0 \\ i & 0 & 0 & i \\ -i & 0 & 0 & i \\ 0 & -i & -i & 0 \end{pmatrix}$
S_x	$\frac{1}{2}\begin{pmatrix} 0 & 1 & 0 & 0 \\ 1 & 0 & 0 & 0 \\ 0 & 0 & 0 & 1 \\ 0 & 0 & 1 & 0 \end{pmatrix}$	$\frac{1}{2\sqrt{2}}\begin{pmatrix} 0 & 1 & 1 & 0 \\ 1 & 0 & 0 & 1 \\ 1 & 0 & 0 & -1 \\ 0 & 1 & -1 & 0 \end{pmatrix}$
$2I_zS_y$	$\frac{1}{2}\begin{pmatrix} 0 & -i & 0 & 0 \\ i & 0 & 0 & 0 \\ 0 & 0 & 0 & i \\ 0 & 0 & -i & 0 \end{pmatrix}$	$\frac{1}{2\sqrt{2}}\begin{pmatrix} 0 & -i & -i & 0 \\ i & 0 & 0 & i \\ i & 0 & 0 & -i \\ 0 & -i & i & 0 \end{pmatrix}$
$\vec{I}\cdot\vec{S}$	$\frac{1}{4}\begin{pmatrix} 1 & 0 & 0 & 0 \\ 0 & -1 & 2 & 0 \\ 0 & 2 & -1 & 0 \\ 0 & 0 & 0 & 1 \end{pmatrix}$	$\frac{1}{4}\begin{pmatrix} 1 & 0 & 0 & 0 \\ 0 & 1 & 0 & 0 \\ 0 & 0 & -3 & 0 \\ 0 & 0 & 0 & 1 \end{pmatrix}$

be found to switch between symmetrical and non-symmetrical Hamiltonians.

Appendix A

To construct the matrix representations of products of angular momentum operators, we start with the Pauli matrices for an isolated spin K = ½, supplemented by the identity operator E_2:

$$K_x = \frac{1}{2}\begin{pmatrix} 0 & 1 \\ 1 & 0 \end{pmatrix}; \quad K_y = \frac{i}{2}\begin{pmatrix} 0 & -1 \\ 1 & 0 \end{pmatrix}; \quad K_z = \frac{1}{2}\begin{pmatrix} 1 & 0 \\ 0 & -1 \end{pmatrix}; \quad E_2 = \begin{pmatrix} 1 & 0 \\ 0 & 1 \end{pmatrix} \tag{A1}$$

For a system with two spins I = ½ and S = ½, one can readily construct a basis consisting of matrix representations of 16 normalized products of angular momentum operators:

Table A2

Transformation of the difference $I_x - S_x$ in the product base Φ_{PB} into the singlet-triplet base Φ_{STB} when the *rf* field is switched on. The two off-diagonal elements in Φ_{STB} correspond to long-lived coherences. The basis kets are in the same order as in Eqs. (3) and (5).

Operator	In Φ_{STB}	Operator	In Φ_{PB}	In Φ_{STB}
$I_x - S_x$	$\frac{1}{\sqrt{2}}\begin{pmatrix} 0 & 0 & -1 & 0 \\ 0 & 0 & 0 & 0 \\ -1 & 0 & 0 & 1 \\ 0 & 0 & 1 & 0 \end{pmatrix}$	$I'_z - S'_z$	$\begin{pmatrix} 0 & 0 & 0 & 0 \\ 0 & 1 & 0 & 0 \\ 0 & 0 & -1 & 0 \\ 0 & 0 & 0 & 0 \end{pmatrix}$	$\begin{pmatrix} 0 & 0 & 0 & 0 \\ 0 & 0 & 1 & 0 \\ 0 & 1 & 0 & 0 \\ 0 & 0 & 0 & 0 \end{pmatrix}$

Table A3

A selection of matrix representations of operators: diagonal elements represent populations and off-diagonal elements ordinary coherences in the product base Φ_{PB} or long-lived coherences (LLC) in the singlet-triplet base Φ_{STB}.

Operator	In Φ_{PB}	In Φ_{STB}
$\|S_0\rangle\langle S_0\|$	$\frac{1}{2}\begin{pmatrix} 0 & 0 & 0 & 0 \\ 0 & 1 & -1 & 0 \\ 0 & -1 & 1 & 0 \\ 0 & 0 & 0 & 0 \end{pmatrix}$	$\begin{pmatrix} 0 & 0 & 0 & 0 \\ 0 & 0 & 0 & 0 \\ 0 & 0 & 1 & 0 \\ 0 & 0 & 0 & 0 \end{pmatrix}$
$\|T_0\rangle\langle T_0\|$	$\frac{1}{2}\begin{pmatrix} 0 & 0 & 0 & 0 \\ 0 & 1 & 1 & 0 \\ 0 & 1 & 1 & 0 \\ 0 & 0 & 0 & 0 \end{pmatrix}$	$\begin{pmatrix} 0 & 0 & 0 & 0 \\ 0 & 1 & 0 & 0 \\ 0 & 0 & 0 & 0 \\ 0 & 0 & 0 & 0 \end{pmatrix}$
$\|T_{-1}\rangle\langle T_{-1}\|$	$\begin{pmatrix} 0 & 0 & 0 & 0 \\ 0 & 0 & 0 & 0 \\ 0 & 0 & 0 & 0 \\ 0 & 0 & 0 & 1 \end{pmatrix}$	$\begin{pmatrix} 0 & 0 & 0 & 0 \\ 0 & 0 & 0 & 0 \\ 0 & 0 & 0 & 0 \\ 0 & 0 & 0 & 1 \end{pmatrix}$
$\|T_{+1}\rangle\langle T_{+1}\|$	$\begin{pmatrix} 1 & 0 & 0 & 0 \\ 0 & 0 & 0 & 0 \\ 0 & 0 & 0 & 0 \\ 0 & 0 & 0 & 0 \end{pmatrix}$	$\begin{pmatrix} 1 & 0 & 0 & 0 \\ 0 & 0 & 0 & 0 \\ 0 & 0 & 0 & 0 \\ 0 & 0 & 0 & 0 \end{pmatrix}$
$\|S_0\rangle\langle T_0\| + \|T_0\rangle\langle S_0\|$	$\begin{pmatrix} 0 & 0 & 0 & 0 \\ 0 & 1 & 0 & 0 \\ 0 & 0 & -1 & 0 \\ 0 & 0 & 0 & 0 \end{pmatrix}$	$\begin{pmatrix} 0 & 0 & 0 & 0 \\ 0 & 0 & 1 & 0 \\ 0 & 1 & 0 & 0 \\ 0 & 0 & 0 & 0 \end{pmatrix}$

$$E = \frac{1}{2} E_2 \otimes E_2;$$
$$I_\mu = K_\mu \otimes E_2;$$
$$S_\mu = E_2 \otimes K_\mu; \qquad\qquad (A2)$$
$$2I_\mu S_\nu = 2K_\mu \otimes K_\nu,$$

where, $\mu, \nu = \{x, y, z\}$. Some examples of product operators that are relevant for this work are shown in Table A1, both in the usual product base Φ_{PB} and in the singlet-triplet base Φ_{STB}.

See Tables A1–A3.

References

[1] M. Carravetta, O.G. Johannessen, M.H. Levitt, Beyond the T_1 limit: singlet nuclear spin states in low magnetic fields, Phys. Rev. Lett. 92 (2004) 153003.

[2] M. Carravetta, M.H. Levitt, Long-lived nuclear spin states in high-field solution NMR, J. Am. Chem. Soc. 126 (2004) 6228–6229.

[3] R. Sarkar, P.R. Vasos, G. Bodenhausen, Singlet-state exchange NMR spectroscopy for the study of very slow dynamic processes, J. Am. Chem. Soc. 129 (2007) 328–334.

[4] G. Pileio, M. Carravetta, E. Hughes, M.H. Levitt, The long-lived nuclear singlet state of N-15-nitrous oxide in solution, J. Am. Chem. Soc. 130 (2008) 12582–12583.

[5] P. Pelupessy, E. Rennella, G. Bodenhausen, High-resolution NMR with unknown spatiotemporal variations of magnetic fields, Science 324 (2009) 1693–1697.

[6] C.A. Meriles, D. Sakellariou, H. Heise, A.J. Moule, A. Pines, Approach to high-resolution ex situ NMR spectroscopy, Science 293 (2001) 82–85.

[7] M. Goldman, Interference effects in the relaxation of a pair of unlike spin-1/2 nuclei, J. Magn. Reson. 60 (1984) 437–452.

[8] H. Shimizu, Theory of the dependence of nuclear magnetic relaxation on the absolute sign of spin–spin coupling constant, J. Chem. Phys. 40 (1964) 3357.

[9] E.L. Mackor, C. MacLean, Sign of J_{HF} in $CHFCl_2$, J. Chem. Phys. 44 (1966) 64.

[10] S. Wimperis, G. Bodenhausen, Relaxation-allowed cross-peaks in two-dimensional NMR correlation spectroscopy, Mol. Phys. 66 (1989) 897–919.

[11] S. Wimperis, G. Bodenhausen, Relaxation-allowed transfer of coherence in NMR between spins which are not scalar coupled, Chem. Phys. Lett. 140 (1987) 41–45.

[12] V. Tugarinov, P.M. Hwang, J.E. Ollerenshaw, L.E. Kay, Cross-correlated relaxation enhanced H-1-C-13 NMR spectroscopy of methyl groups in very high molecular weight proteins and protein complexes, J. Am. Chem. Soc. 125 (2003) 10420–10428.

[13] R. Sarkar, P. Ahuja, P.R. Vasos, G. Bodenhausen, Long-lived coherences for homogeneous line narrowing in spectroscopy, Phys. Rev. Lett. 104 (2010) 053001.

[14] G. Pileio, M. Carravetta, M.H. Levitt, Extremely low-frequency spectroscopy in low-field nuclear magnetic resonance, Phys. Rev. Lett. 103 (2009) 083002.

[15] I. Bertini, M. Fragai, C. Luchinat, G. Parigi, H-1 NMRD profiles of diamagnetic proteins: a model-free analysis, Magn. Reson. Chem. 38 (2000) 543–550.

[16] A.S. Bornet, R. Sarkar, G. Bodenhausen, Life-times of long-lived coherences under different motional regimes, J. Magn. Reson. 206 (2010) 154–156.

[17] R.R. Ernst, G. Bodenhausen, A. Wokaun, Principles of Nuclear Magnetic Resonance in One and Two Dimensions, Oxford University Press, Oxford, 1987.

[18] J. Cavanagh, W.J. Fairbrother, A.G. Palmer, M. Rance, N.J. Skelton, Protein NMR Spectroscopy: Principles and Practice, Elsevier Science, 2007.

[19] M.H. Levitt, L. Dibari, Steady-state in magnetic-resonance pulse experiments, Phys. Rev. Lett. 69 (1992) 3124–3127.

[20] P. Ahuja, R. Sarkar, P.R. Vasos, G. Bodenhausen, Molecular properties determined from the relaxation of long-lived spin states, J. Chem. Phys. 127 (2007) 134112.

[21] R. Sarkar, D. Moskau, F. Ferrage, P.R. Vasos, G. Bodenhausen, Single or triple gradients?, J Magn. Reson. 193 (2008) 110–118.

[22] R. Sarkar, P. Ahuja, D. Moskau, P.R. Vasos, G. Bodenhausen, Extending the scope of singlet-state spectroscopy, ChemPhysChem 8 (2007) 2652–2656.